Reduction of Bass-Reflex Port Nonlinearities by Optimizing the Port Geometry 4661 (P7-3)

N.B. Roozen
Philips Research Labs Eindhoven The Netherlands

J.E.M. Vael
Philips Research Labs Eindhoven The Netherlands

J.A.M. Nieuwendijk
Philips ASA Labs Eindhoven The Netherlands

Presented at the 104th Convention 1998 May 16-19 Amsterdam

AN AUDIO ENGINEERING SOCIETY PREPRINT

Reduction of bass-reflex port nonlinearities by optimizing the port geometry

N.B. Roozen, J.E.M. Vael, J.A.M. Nieuwendijk
Philips Research Laboratories
Prof. Holstlaan 4, 5656AA Eindhoven, the Netherlands
e-mail: roozen@natlab.research.philips.com

Bass-reflex ports are used to enhance the bass reproduction of loudspeakers. However, at higher output levels, the bass-reflex port nonlinearities, specifically the unsteady separation of the acoustic flow, can lead to blowing sounds and acoustic losses.
Calculations and measurements are presented for a number of port geometries. The effect of rounding the port terminations and the effect of converging-diverging ports on the production of blowing sounds are investigated. It appears that the intensity of the unsteady separation of the acoustic flow, as well as the radiation efficiency of the port and the quality factor of the port resonances, altogether determine the level of blowing noise. Maximum reduction of the blowing sounds and acoustic losses is obtained by using a port contour geometry that slowly diverges from the centre towards both port ends and is rounded with curvature radii that are not too large at both port terminations.

0 Introduction

Bass-reflex ports are commonly used to achieve more low frequency output in loudspeakers. Without a port, the loudspeaker box volume would have to be much larger to generate the same acoustic performance in the low frequency range.

At higher sound levels a bass-reflex port can lead to blowing sounds. The blowing sounds are generated by aero-dynamic phenomena which occur at the port terminations. Especially small loudspeaker cabinets suffer from these unwanted blowing noises.

In the literature a number of studies have been reported on this topic. It is generally recognized that a larger port cross-sectional area is better than a smaller cross-section having the same Helmholtz frequency, as the acoustic flow amplitude is smaller. It is also generally recognized that edges should be smooth and discontinuities in the port contour should be avoided.

Backmann performed an extensive study on a number of ports, such as ports with different types of flanges and bends [1]. He concluded that both the inner and outer port ends should be designed to reduce the blowing sounds. Rounding only one port end reduces these blowing

sounds slightly; therefore both port ends need to be rounded for maximum reduction in blowing sound.

The approach which was chosen to reduce the blowing sounds by the authors of this paper was to increase the cross-sectional area of the port towards the port ends while maintaining a certain acoustic mass m_a and the same physical port length L. These conflicting requirements can be partly fulfilled by making use of tapered or converging-diverging ports [2], [3], [4]. It is essential to widen the port towards both port ends, as the acoustic flow oscillates from inwards to outwards and vice versa.

Numerical simulations and experimental investigations are presented. It is shown that the blowing sounds can be attributed to the unsteady separation of the acoustic flow at the port end. It was found that this separation results in an impulsive excitation of the $\lambda/2$-mode in the longitudinal direction of the port and its harmonics, where λ denotes the acoustic wavelength. The effect that rounding the port ends using different curvature radii has on the production of blowing sounds was examined, as has the effect of converging-diverging port cross sections. It is also shown that the widening-angle of the port should not be made too large to avoid flow separation within the port.

Recently, Vanderkooy [5] published some interesting work in this field. He derived closed form solutions for the Helmholtz frequency of hyperbolic and cosine-hyperbolic port geometries. He also did an extensive experimental study, from which he concluded that the losses occurring in the port very much affect the net result of the port. From the present paper it will become clear that these port losses are due to a dissipation of acoustic energy by convective effects.

1 Bass-reflex port applied to small boxes

Application of a bass-reflex port to small loudspeaker boxes implies that the cross-sectional port radius has to be relatively small in order to achieve a sufficiently low Helmholtz frequency. This can easily be seen from the expression for the Helmholtz frequency (see [6] or [7]):

$$f_{Helmholtz} = \frac{c}{2\pi}\sqrt{\frac{S_0}{L_{eff}V}} = \frac{c}{2\pi}\sqrt{\frac{\rho_0}{m_a V}}\,, \tag{1}$$

where c is the speed of sound, ρ_0 is the mean density of air, S_0 is the reference cross-sectional area of the port, V is the volume of the box, L_{eff} is the effective port length defined as

$$L_{eff} = \int_0^L \frac{S_0}{S(x)}dx\,, \tag{2}$$

and m_a is the acoustic mass of the port defined as

$$m_a = \int_0^L \frac{\rho_0}{S(x)}dx\,. \tag{3}$$

In these equations L is the physical length of the port, x is the axial coordinate along the port axis and $S(x)$ is the cross-sectional area of the port at axial coordinate x. In the calculation

of the effective length L_{eff} and the acoustic mass m_a of the port, end corrections should be *additionally* accounted for. Appropriate end corrections can be found in the literature [6], [7], [8]. Closed form solutions for the effective length L_{eff} are given by Vanderkooy for a number of port shapes [5].

A smaller box volume V forces the port cross-sectional area S_0 to become smaller for a given physical port length L and a given Helmholtz frequency $f_{Helmholtz}$. This means that for small boxes, with a relatively small cross-sectional area S_0, the acoustic flow velocity in the port is relatively high. The acoustic flow velocity amplitudes can easily amount 10 m/s or more (see table 1).

Table 1: Required acoustic flow velocity for a cylindrical port with specifications as given in the table, fluid density of air taken to be 1.2 kg/m^3.

Cross-sectional radius	1 cm,
Helmholtz frequency	50 Hz,
sound pressure level in free field at 1 m distance	70 dB.
Required volume flow (RMS)	2.3 l/s,
required acoustic flow velocity amplitude	10 m/s.

As a result of these high air velocities, bass-reflex ports applied to small loudspeaker boxes often lead to blowing sounds due to airflow nonlinearities. As will be seen later, these blowing sounds can be subdivided into broadband noise and pure tones caused by port resonances.

2 Deterministic nature of the blowing sounds

Two mechanisms can be hold responsible for the production of the blowing sounds: boundary layer turbulence and unsteady separation of the acoustic flow at the port termination. The dimensionless parameters which determine the probability of occurrence of these mechanisms are the Reynolds number Re_δ, based on the boundary layer thickness δ, and the Strouhal number St.

The Reynolds number Re_δ based on the boundary layer thickness δ is defined as (see [9], [10] or [11])

$$Re_\delta = \frac{u\delta}{\nu}\,, \tag{4}$$

where the boundary layer thickness $\delta = \sqrt{(2\nu/\omega)}$. Here ν is the kinematic viscosity, ω is the angular frequency and u is the acoustic flow velocity.

The critical Reynolds number Re_δ for a boundary layer on a flat plate equals $Re_{\delta\_crit} = 520$ [9]. For Reynolds numbers larger than 520, the boundary layer will become turbulent. Merkli [10] gives critical Reynold numbers Re_δ which vary between 500 and 1000. In table 2 the critical velocity of the acoustic flow in the port and the critical sound pressure level at a distance of 1 m in free field for occurrence of boundary layer turbulence is given for a specific situation.

Table 2: Critical velocity and sound pressure level for a bass-reflex port with a cross-sectional port radius a=1 cm that is tuned to a Helmholtz frequency of 45 Hz, the kinematic viscosity of air taken to be $\nu = 15 \cdot 10^{-6}$ m^2/s.

	Critical velocity of the acoustic flow	Critical SPL at 1 m in free field
Boundary layer turbulence	25 m/s	78 dB
Unsteady flow separation	3 m/s	60 dB

The Strouhal number is a measure for the ratio of the acceleration caused by the unsteadiness of the flow and the convective acceleration caused by the non-uniformity of the flow at the port termination. It is defined as the ratio of the cross-sectional port radius a and the particle displacement u/ω:

$$St = \omega a/u. \tag{5}$$

If the particle displacement u/ω approaches the order of the port radius a, i.e. if St is of the order 1 or smaller, then there will be an unsteady separation of the acoustic flow at the port end, vortices associated with the separation of the flow will form, and jets will form (see [12]).

In figure 1, the physical phenomena occurring during inflow and outflow are sketched for low Strouhal numbers. Jet formation occurs at outflow, while a sink-like flow takes place at inflow.

In table 2 the critical velocity of the acoustic flow in the port and the critical sound pressure level at a distance of 1 m in free field for occurrence of unsteady flow separation of the acoustic flow at the port end is given for a specific situation.

For small bass-reflex ports (port cross-sectional radius a=1 cm) it can be concluded that unsteady separation of the acoustic flow and the associated free jet formation will be rather common. The jet formation results in impulsive excitation of the resonance of the $\lambda/2$-mode in the longitudinal direction of the port and its harmonics (see [3]). Broadband jet turbulence or boundary layer turbulence is expected to become relevant only at very high pressure levels.

The noise spectrum which was measured at a distance of 1 m for a cylindrical bass-reflex port with a physical length L=0.13 is shown in figure 2. The impulsively excited $\lambda/2$ acoustic resonance at $c/(2L') \approx 1100$ Hz was observed, where L' is the physical length L corrected for end effects. The harmonics of the $\lambda/2$ resonance were also excited, but less strongly than the fundamental bass-reflex port mode at 1100 Hz.

Although the loudspeaker was driven by an electrical signal with a frequency of 45 Hz only, harmonics of 45 Hz were also present. These harmonics, which are all at least 20 dB below the 45 Hz signal, are caused by harmonic distortion of the loudspeaker itself. This was confirmed by separate measurements of the loudspeaker response.

The resonance peak at 1100 Hz is rather wide, which indicates that the resonance is strongly damped. At low velocity amplitudes the damping of the 1100 Hz resonance is mainly due to acoustic radiation into open space. The quality factor Q, which is defined as the resonance

frequency divided by the half power bandwidth of the resonance (-3 dB bandwidth), reduces at higher amplitudes because acoustic energy is dissipated by convective effects [3].

3 Numerical simulations

In this section the numerical analysis results of the unsteady airflow through a bass-reflex port are discussed. The flow is described by the unsteady full Navier-Stokes equations. The objective of these calculations is to assess the effect of changes in the port geometry on the flow separation and the associated vortex production. The vorticity production is directly related to the flow separation.

The advantage of using a numerical prediction model is that the physics of the airflow through the port can be understood very well. Experimental observation of the details of this flow separation is extremely difficult. From the numerical calculations the points in the flow at which vortices are generated and their intensities can be revealed. Based on these results a better port design can be made.

The model used is axi-symmetric. In figure 4 the 2D-axi-symmetric mesh of a cylindrical port with a curvature radius of 2 cm (port C) is presented. In table 3 some statistics of the model can be found. The middle part of the model represents the bass-reflex port with rounded ends. The left and right parts are used to let the airflow enter and leave the finite-element domain. These parts are chosen long enough to ensure that the boundary conditions at the left and right end do not influence the airflow too much.

At the left end of the finite element domain, a time-varying sinusoidal air velocity in the axial direction is prescribed. On the finite element boundary at the bottom, which lies on the line of axi-symmetry, the air is allowed to flow in the axial direction only. At the finite element boundary at the top, the air velocity in both the R and Z directions are set to zero (no-slip condition). At the right end of the finite element domain, the air is free to flow in both the R and Z directions.

For a bass-reflex port tuned to a Helmholtz frequency of 45 Hz and the kinematic viscosity of air taken to be $\nu = 15 \cdot 10^{-6}$ m^2/s, the boundary layer thickness is of the order of $\delta = \sqrt{(2\nu)/\omega} = 0.3$ mm, which is very thin. In order to represent the flow gradients in this boundary layer accurately, ten linear elements are used across the boundary layer. In the port, a total of 60 linear elements is used in the radial direction.

The flow is considered to be locally incompressible. This is valid because the Helmholtz number $He = a/\lambda$ of the flow is small enough. At 45 Hz the wave propagation is negligible compared to the dimensions of the object.

Compressibility effects in the port can be neglected if the square of the Mach number, M^2, is sufficiently small compared to unity. The Mach number M is defined as $M = u/c$. In the present case $M^2 < 10^{-2}$. Note, however, that the flow in the loudspeaker box (which is not accounted for by the numerical model) is essentially compressible.

4 Results of numerical simulations

A number of different port geometries were analysed as shown in figure 3. For a fair comparison between the ports, both the physical length of the ports and the acoustic mass m_a of the ports are kept the same. The latter means that the Helmholtz resonances of the box-port combinations are the same. In order to obtain ports with the same acoustic mass m_a for a given contour shape and a fixed port length, the smallest diameter of the port is varied, the acoustic mass of the port is calculated with a dedicated software program, and the required smallest diameter of the port is calculated iteratively. Therefore a port which has a rather large outer diameter (such as the parabolic shaped port, Port D, see figure 3) will have a rather small diameter at its centre in order to get the same acoustic mass.

The numerical calculations of the flow through a port were performed for a number of different volume flows. Only the calculations for which an RMS volume flow of 2.22 l/s at the inlet is prescribed are shown. This volume flow is close to the maximum volume flow which can be simulated with the present model. Calculations for much higher volume flows diverge because the mesh size is not sufficiently small to resolve the details of the flow. An RMS volume flow of 2.22 l/s corresponds to a sound pressure level of 70 dB at 1 m distance for radiation into free space. In this case, the airflow velocity amplitude equals 10 m/s for a cylindrical port with a cross-sectional radius a= 1 cm. At the inlet of the mesh domain a sinusoidal velocity in the axial direction is prescribed with a frequency of 50 Hz. The numerical simulations were performed for 20 ms, corresponding to one cycle.

A detailed view of the velocity vectors and vorticity contours during outflow of port C can be seen in figure 5. The vorticity $\vec{\omega}$, which is defined as $\vec{\omega} = \nabla \times \vec{v}$, is a direct measure for the strength of the vortex. In the figures, the vorticity in the circumferential direction is shown (the other components of the vorticity vector vanish as a result of axi-symmetry). Vortices are generated at the outlet, as a result of flow separation. It is this flow separation which causes the impulsive excitation of the $\lambda/2$ acoustic port resonance.

In figures 6 – 9 the vorticity production of port C and port E are shown for subsequent moments in time. It can be seen that a vortex develops at the port termination. The vortex is generated during the deceleration phase of the outflow. Even though the flow has reversed its direction after t=10 ms, a vortex remains present.

The vorticity levels occurring in the centre of the vortex are tabulated in table 4 for different moments in time and different port geometries. As can be seen from this table, the vortex intensity of a cylindrical port with a curvature radius of 5 mm (port A) is smaller than the vortex intensity of a cylindrical port with a curvature radius of 20 mm (port C). By applying a converging-diverging geometry combined with a curvature radius of 5 mm (port E), the vortex intensity can be reduced further. In this case, the vortex intensity is reduced by a factor of two compared to that of port C; see table 4. This reduction in the local velocity is due to an increased port cross-section at the outlet of the port.

It is also interesting to see what happens if the port cross-section varies too fast. Port D is a port geometry with a rather strong converging-diverging cross-section, as shown in figure 3. In such a case the flow is not able to adhere to the port wall. It appeared that at a volume flow of 2.22 l/s, vortices are produced in the middle of the port, as can be seen in figure 10.

Besides that, the vortex is strong as a result of the fact that the port is narrow at the middle of the port (see table 4). The fact that flow separation takes place *inside* the port is highly undesirable. In such a situation, the vortices will accumulate inside the port, resulting in a highly distorted sound production and much broadband noise caused by turbulence.

5 Experimental investigation

Experimental investigations were performed for the ports as shown in figure 3. Additionally, a cylindrical port with sharp edges was examined. This port will be denoted by "port 0". All port geometries are designed to have the same acoustical mass of about m_{ap}=300 kg/m^4. In reality, however, the acoustical mass differs slightly between the ports as a result of geometric inaccuracies.

Moreover, it appeared that the acoustical mass m_{ap} decreases slightly with increasing sound pressure level. This change in the acoustical mass m_{ap} is due to the fact that at higher sound pressure levels the air velocity in the port increases, which results in flow separation. At higher amplitudes the point of separation moves to a smaller cross-sectional radius, thus reducing the effective length of the port. See ref [4] for a quantification of this effect.

The fact that the acoustic mass m_a does not change very much for the port with sharp ends is logical; the point of separation is predetermined for such a port.

In a reverberant room of 227 m^3 the blowing sounds which are produced by the ports were measured. A bandpass loudspeaker system was used for this purpose, as shown in figure 11. With this measurement set-up, the sounds which are produced by the port only can be measured well. The loudspeaker cannot easily radiate sound directly into the measurement room.

The amount of blowing sound was measured in the frequency range between 100 Hz and 10 kHz for different driving frequencies and different levels. The sound power levels correspond to 85, 90 and 95 dB

A first observation is that, as expected, there were three kinds of unwanted sounds (see figure 2): harmonic distortion (for frequencies up to about 500 Hz), broadband noise and the $\lambda/2$-port resonance. The harmonic distortion is mainly attributed to the loudspeaker itself. Broadband noise is due to the inherent broadband nature of the jet sounds. The impulsively excited port resonance occurs at a frequency of about 1.1 kHz, which corresponds well with the $\lambda/2$ acoustic resonance of a port with a physical length of 13 cm after appropriate end corrections have been taken into account, i.e. $f = c/(2L')$.

The A-weighted sound power of the blowing sounds (including the harmonic distortion) for driving levels corresponding to a sound power level at the driving frequency (45 Hz) of 85, 90 and 95 dB are shown in figure 14.

The amount of blowing sounds which are produced by the ports appears to be strongly dependent upon the level of excitation. Obviously, the amount of blowing sounds increases at higher levels. More subtle, however, is that at low levels a cylindrical port with a large curvature radius produces less blowing sound than a cylindrical port with a small curvature

radius, while at higher levels it is the other way around.

Let us consider the cylindrical ports first. Port 0 is a cylindrical port with a sharp end and ports A, B, and C are cylindrical ports with a curvature radius of R=5 mm, R=10 mm and R=20 mm, respectively. From figure 14 it can be seen that at low levels (L_W = 85 dB at 45 Hz) a port with a large curvature radius (port C, for instance) produces less blowing sound, while at high levels (L_W = 95 dB at 45 Hz) a port with a small curvature radius (port A or even the port with a sharp edge, port 0) produces less blowing sound. At other driving frequencies the same tendency was found.

At low levels (L_W = 85 dB at 45 Hz) a port with a larger curvature radius produces less blowing sound because the vortex is less intense. However, from the numerical simulations it was concluded that port A (curvature radius 5 mm) produces a less intense vortex than port C (curvature radius 20 mm). Most probably the reason that port C produces less blowing sound than port A according to the measurements (see figure 14) is that a port with a larger curvature radius radiates noise less efficiently.

In order to understand what is happening at high velocities, it must be understood that the production of blowing sounds depends not only upon the vortex intensity but also upon the quality factor of the port, i.e. the amount of damping of the port resonance. For low velocity amplitudes the quality factor of the port is determined by the amount of acoustic radiation (which in turn is determined by the acoustic impedance of the port). At low velocity amplitudes, the quality factor is approximately the same for all ports. At higher levels energy is transfered from the acoustic oscillation of the port (at about 1 kHz) to the free jet formed during the vortex shedding at the driving frequency, which reduces the quality factor significantly. This transfer of energy is strongest when the acoustic oscillation can interact with the free jet. In first order approximation the energy losses are proportional to the flow velocity on the jet [12].

Furthermore, it appears that this type of interaction is strongly reduced for ports with large curvature radii. In some cases one can even find a net energy production (whistling) rather than absorption [12]. At high air velocities, the quality factor of a port with a small curvature radius or even a port with sharp ends is significantly smaller than the quality factor of a port with a large curvature radius. Additional measurements confirmed a reduction of the quality factor at higher driving levels. Apparently, at high air velocities a cylindrical port with a large curvature radius produces more blowing sounds than a cylindrical port with a small curvature radius, even if the source of sound is weaker. This indicates that the increase in quality factor with curvature radius compensates the reduction of sound source and radiation efficiency at high amplitudes.

Vanderkooy [5] also found that a cylindrical port with a large curvature radius (curvature radius R about twice the port cross-sectional radius a) can produce more blowing sounds than a cylindrical port with sharp port ends. He explained this behaviour by reasoning that there are less losses at the edges for a port with a large curvature radius. A better explanation, however, is that the damping of the $\lambda/2$ port resonance is strongly increased for a port with sharp edges as a result of a dissipation of acoustic energy by convective effects.

The effect of the curvature radii for a cylindrical port at low and high driving levels can be seen in figure 14 (ports 0, A, B and C).

Now that the effect of different curvature radii for cylindrical ports has been discussed, the effect of a non-cylindrical port geometry, such as that of port D and port E, will be considered. It can be seen from figure 14 that port D, which is strongly parabolic, produces high levels of blowing sounds. This can be explained by what was found from the numerical simulations of the preceding section. With the numerical simulations it was found that for such a port contour, the vortices are created *inside* the port. This is highly undesirable because in such a situation the vortices will accumulate inside the port, resulting in strong broadband turbulent sound production. The type of blowing sounds which are produced by this port is also different from that of the other ports. In figure 12 the spectrum of port D is shown.

By slowly converging and diverging the port geometry, like the geometry of port E, the flow is able to adhere to the port wall. This prevents separation *inside* the port, while at the same time the cross-sectional area of the port towards the port ends is increased compared to a cylindrical port with the same acoustic mass m_a. The increased cross-sectional area reduces the local air velocity and therefore also reduces the vortex intensity and the associated production of blowing sounds. This was also concluded from the numerical simulations; port E produces a less intense vortex than port C (see table 4). Furthermore, at high acoustic levels port E produces less blowing sound compared to the other ports.

As can be seen from figure 14, the blowing sounds of port E are the lowest of all ports for all levels tested. Compared to a cylindrical port with the same curvature radius (port A), port E produces 1 dB, 4 dB and 5.5 dB less blowing sound for a sound power level of 85, 90 and 95 dB, respectively, which is in agreement with the numerical simulations.

6 Conclusions

It was found that there are two kinds of blowing sounds which can be attributed to the unsteady separation of the acoustic flow at the port end, i.e. broadband noise and the $\lambda/2$-port resonance. The $\lambda/2$-port resonance is impulsively excited by the periodic separation of the acoustic flow.

The blowing sounds can be reduced by designing the port geometry such that the strength of the vortices caused by flow separation and jet forming at the end of the port during the deceleration phase of the flow is minimal. Reducing the vortex strengths reduces the production of blowing sounds, causes less acoustic energy to be dissipated by the vortices and therefore also improves the reproduction of the primary noises.

A better understanding of the very complex phenomena which occur at the port termination was obtained from the numerical simulations. The points in the flow at which vortices are generated and their intensities were revealed. From these simulations it was concluded that the vortex strength is minimal for a slowly converging-diverging port geometry with a small curvature radius at both port ends. A strongly converging-diverging port geometry is expected to produce much blowing sound. It was also found that the vortex is generated during the deceleration phase of the outflow.

From the experimental investigations it was found that not only the vortex strength and vortex location are important, but also the sound radiation efficiency and the quality factor of the $\lambda/2$ port resonance (and its harmonics). It appears that for a sharp edged port as well as for a port with a small curvature radius the quality factor of the $\lambda/2$ port resonance drops significantly with increasing driving levels. The quality factor of the port becomes smaller as a result of the transfer of energy from the acoustic oscillation of the port to the free jet formed during the vortex shedding at the driving frequency. For this reason, both a sharp edged cylindrical port and a cylindrical port with a small curvature radius produce less blowing sound at higher driving levels than a cylindrical port with a large curvature radius. The curvature radius should therefore not be made too large.

A port contour which combines a reduction of the vortex strength with a low quality factor at high driving levels is a port contour which slowly diverges towards both port ends with a maximum angle of 6 degrees (measured from port contour to port axis) and which is rounded with relatively small curvature radii at both port ends (see figure 3, port E). Compared to a cylindrical port with the same curvature radius, this "optimal" port produces 1 dB, 4 dB and 5.5 dB less blowing sound for a sound power level of 85, 90 and 95 dB, respectively.

References

[1] J. Backman, "The nonlinear behaviour of reflex ports", presented at 98th AES Convention, Paris, 1995 February 25-28, preprint #3999.

[2] European patent, EP appln. nr. 97202358.4, "Loudspeaker system having a bass-reflex port", first filing date 1997, July 26.

[3] N.B. Roozen, M. Bockholts, P. van Eck, and A. Hirschberg, "Vortex sound in bass-reflex ports of loudspeakers, Part I: Observation of response to harmonic excitation and remedial measures." Submitted to the Journal of Acoustical Society of America.

[4] N.B. Roozen, M. Bockholts, P. van Eck, and A. Hirschberg, "Vortex sound in bass-reflex ports of loudspeakers, Part II. A method to estimate the point of separation." Submitted to the Journal of Acoustical Society of America.

[5] J. Vanderkooy, "Loudspeaker ports", presented at 103rd AES Convention, New York, 1997 September 26-29, preprint #4523.

[6] J. Merhaut, *Theory of electroacoustics* (McGraw-Hill, 1981).

[7] L.L. Beranek, *Acoustics* (McGraw-Hill, 1954).

[8] A. Cummings, "Acoustics of a wine bottle", Journal of Sound and Vibration, **31**, 331-343 (1973).

[9] H. Schlichting, *Boundary-Layer Theory*, (McGraw-Hill, 1979, Seventh Edition)

[10] P. Merkli, "Theoretische und experimentelle thermoakustische Untersuchungen am Kolbengetriebenen Resonanzrohr", PhD thesis, Eidgenossische Technische Hochschule Zurich (1973).

[11] P. Merkli and H. Thomann, "Transition to turbulence in oscillating pipe flow", J.Fluid Mech., **68** (3), 567-575 (1975).

[12] M.C.A.M. Peters, A. Hirschberg, A.J. Reijnen and A.P.J. Wijnands, "Damping and reflection coefficient measurements for an open pipe at low Mach and low Helmholtz numbers", J.Fluid Mech., **256**, 499-534 (1993).

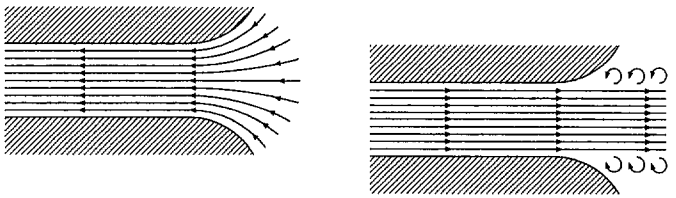

Figure 1: *Sink-like inflow* (***left***) *and jet-like outflow* (***right***).

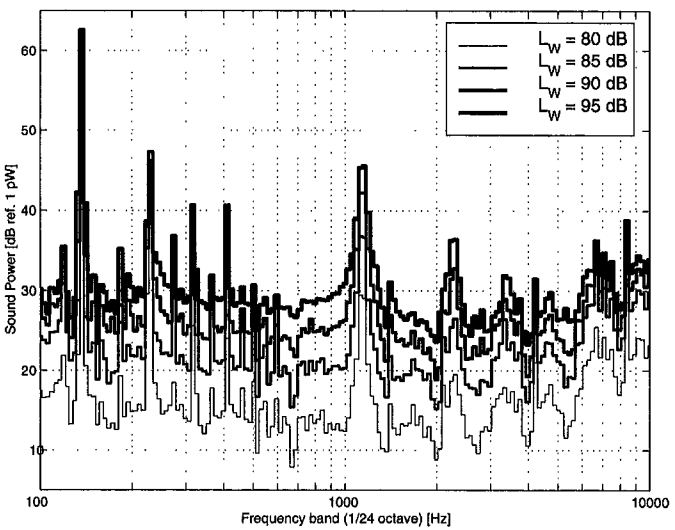

Figure 2: *Sound power of blowing sounds of a cylindrical bass-reflex port with sharp edges (port 0) for the sound power levels 80, 85, 90 and 95 dB at the driving frequency. Physical port length L=0.13 m. port cross-sectional radius a=0.014 m, Loudspeaker driven with a single frequency of 45 Hz.*

port A

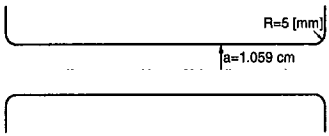

port B

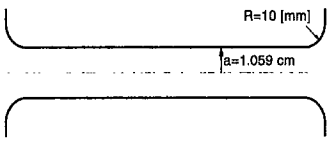

port C

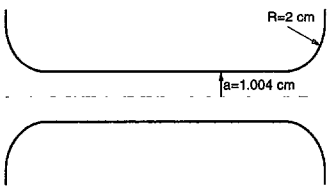

port D

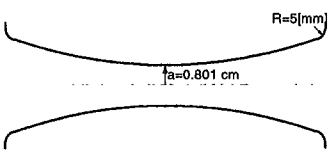

port E

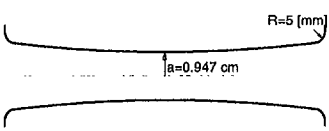

Figure 3: Port geometries.

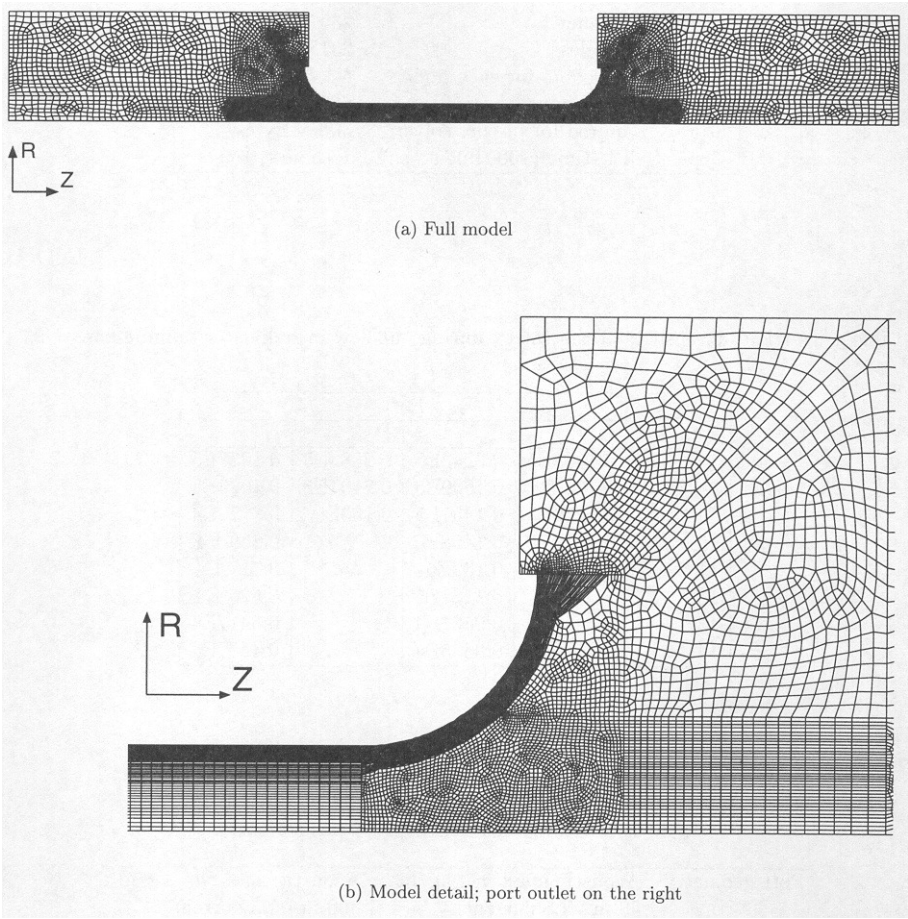

Figure 4: *Numerical model for cylindrical port with a curvature radius of 2 cm (port C).*

Table 3: Model statistics.

Geometry:	2D-axisymmetric
Number of elements:	23570
Number of nodes:	23180
Degrees of freedom for each node:	U_r, U_z, P
number of equations:	68370
Storage required for in-core solver:	300 MBytes
Typical CPU-time (100 time-steps):	13 hours

Table 4: Vorticity intensities of the vortex during out-flow in radians/s, volume flow = 2.22 l/s.

Time	Port			
step, ms	A	C	D	E
7	0.1558E5	0.2242E5	0.2883E5	0.1027E5
8	0.125 E5	0.1609E5	0.2104E5	0.1023E5
9	0.1279E5	0.1451E5	0.163E5	0.8776E4
10	0.1074E5	0.1458E5		0.839 E4
11		0.132E5		0.717 E4
12		0.1181E5		0.626 E4
13		0.9527E4		0.5417E4
14		0.8535E4		0.4481E4

Table 5: Measured acoustic mass of various ports.

Port geometry	Acoustic mass m_a, kg/m^4, 50 mA LS current	Acoustic mass m_a, kg/m^4, 800 mA LS current
0	278	275
A	305	297
C	309	283
E	324	309

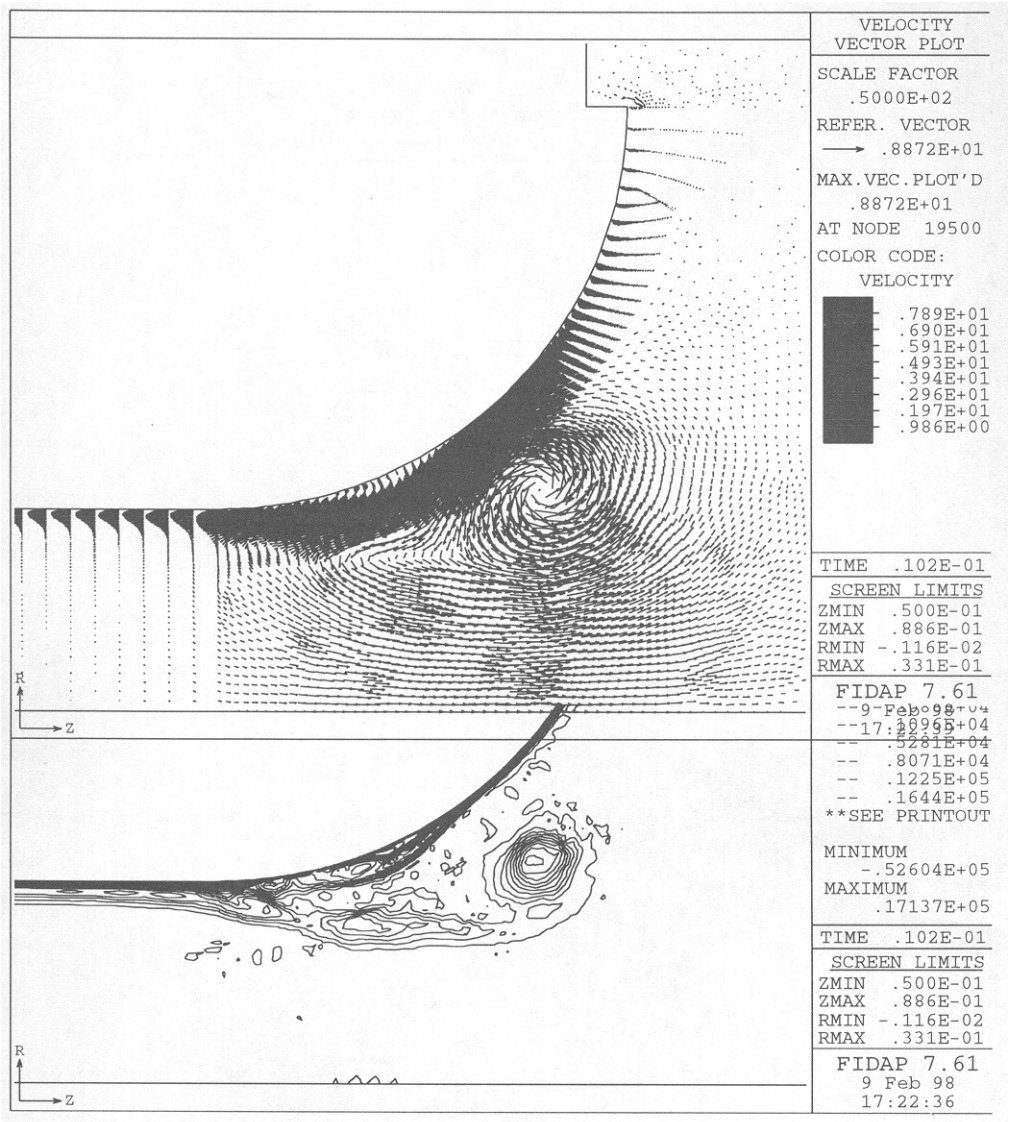

Figure 5: *Velocity vectors and vorticity contours at the outlet of port C, 2.22 l/s, at time t=10.2 ms (one cycle equals 20 ms).*

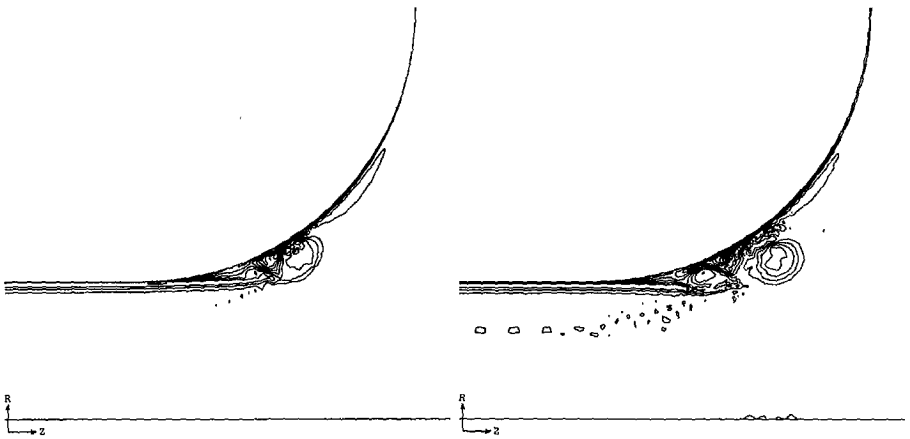

(a) time t=7 ms (maximum vorticity in vortex 0.2242E5 radians/s)

(b) time t=8 ms (maximum vorticity in vortex 0.1609E5 radians/s)

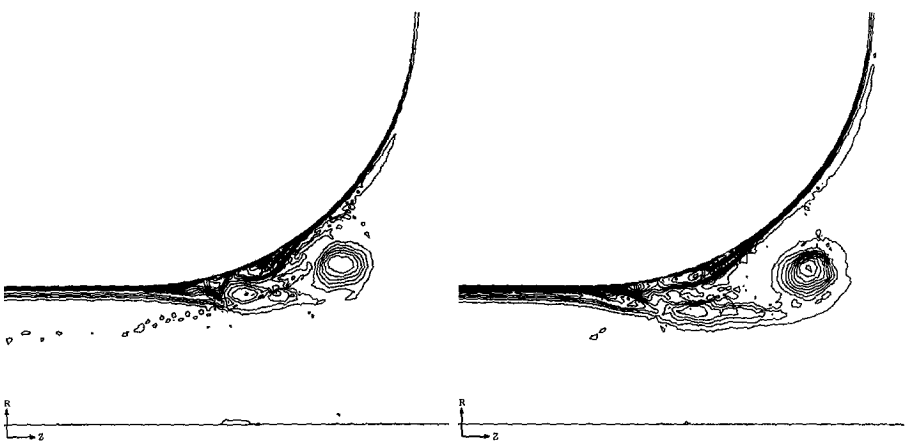

(c) time t=9 ms (maximum vorticity in vortex 0.1451E5 radians/s)

(d) time t=10 ms (maximum vorticity in vortex 0.1458E5 radians/s)

Figure 6: *Vorticity contours at the outlet of port C, 2.22 l/s, time t=7..10 ms.*

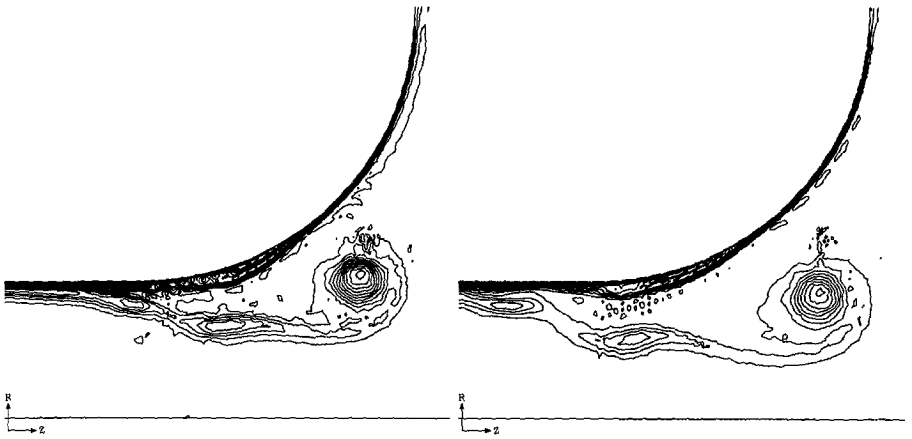

(a) time t=11 ms (maximum vorticity in vortex 0.132E5 radians/s)

(b) time t=12 ms (maximum vorticity in vortex 0.1181E5 radians/s)

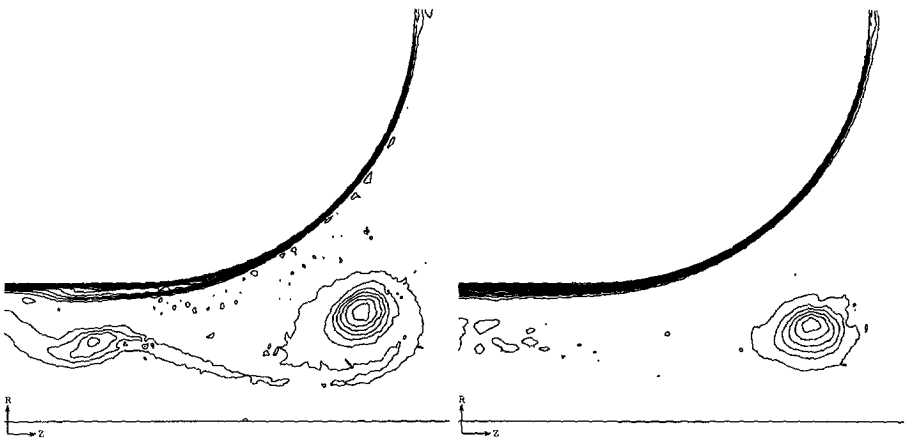

(c) time t=13 ms (maximum vorticity in vortex 0.9527E4 radians/s)

(d) time t=14 ms (maximum vorticity in vortex 0.8535E4 radians/s)

Figure 7: *Vorticity contours at the outlet of port C, 2.22 l/s, time t=11..14 ms.*

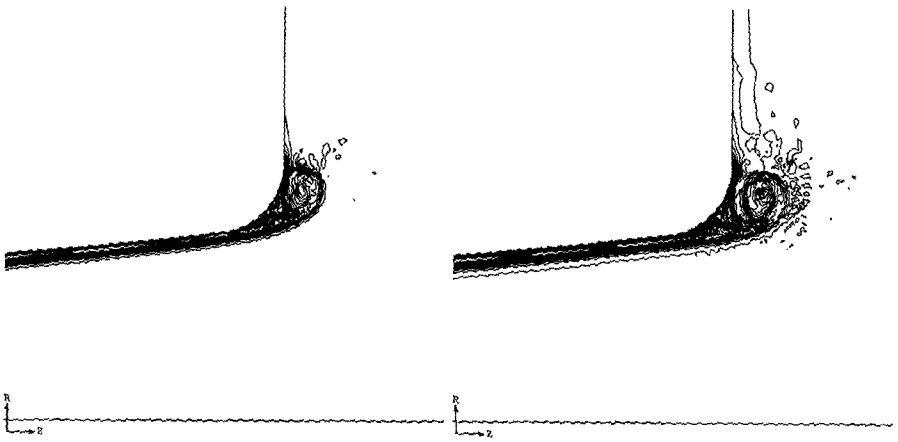

(a) time t=7 ms (maximum vorticity in vortex 0.1027E5 radians/s)

(b) time t=8 ms (maximum vorticity in vortex 0.1023E5 radians/s)

(c) time t=9 ms (maximum vorticity in vortex 0.8776E4 radians/s)

(d) time t=10 ms (maximum vorticity in vortex 0.839E4 radians/s)

Figure 8: *Vorticity contours at the outlet of port E, 2.22 l/s, time t=7..10 ms.*

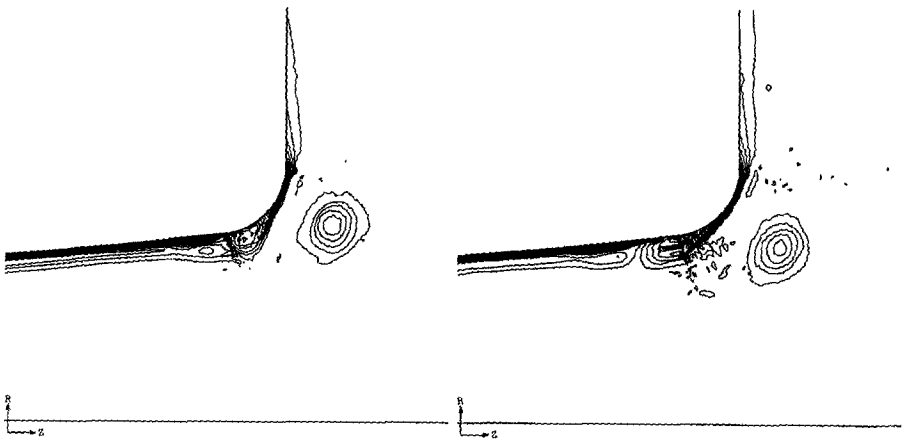

(a) time t=11 ms (maximum vorticity in vortex 0.717E4 radians/s)

(b) time t=12 ms (maximum vorticity in vortex 0.626E4 radians/s)

(c) time t=13 ms (maximum vorticity in vortex 0.5417E4 radians/s)

(d) time t=14 ms (maximum vorticity in vortex 0.4481E4 radians/s)

Figure 9: *Vorticity contours at the outlet of port E, 2.22 l/s, time t=11..14 ms.*

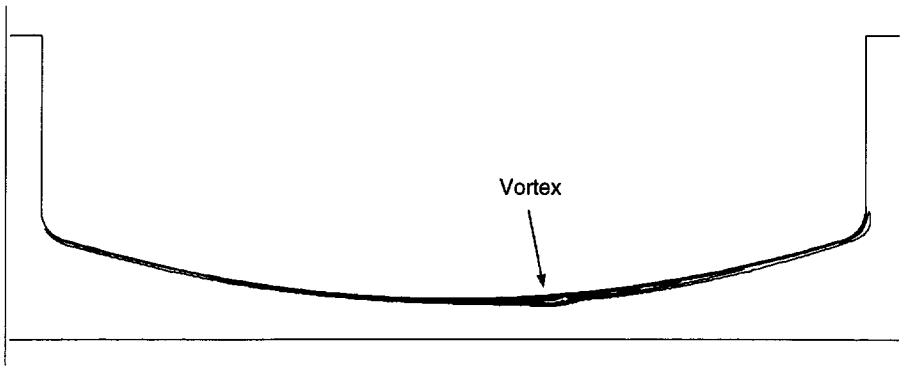

(a) Full model view

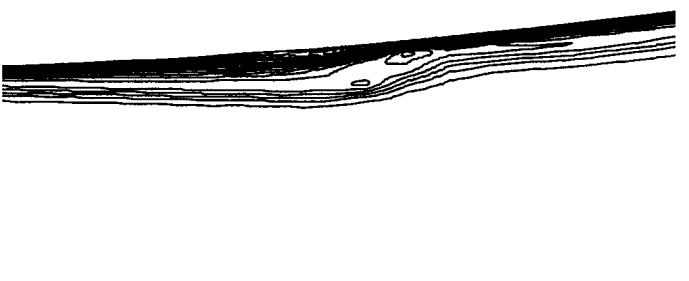

(b) Zoomed view

Figure 10: *Vorticity contours of port D, 2.22 l/s, time t=10 ms.*

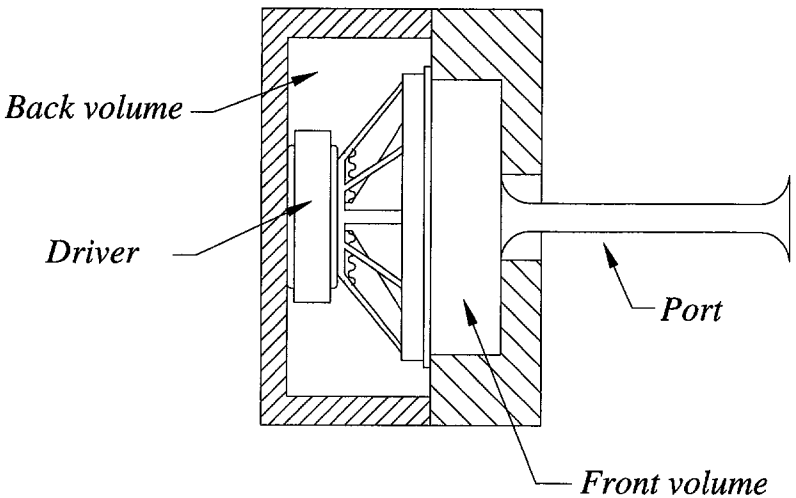

Figure 11: *Band-pass loudspeaker system.*

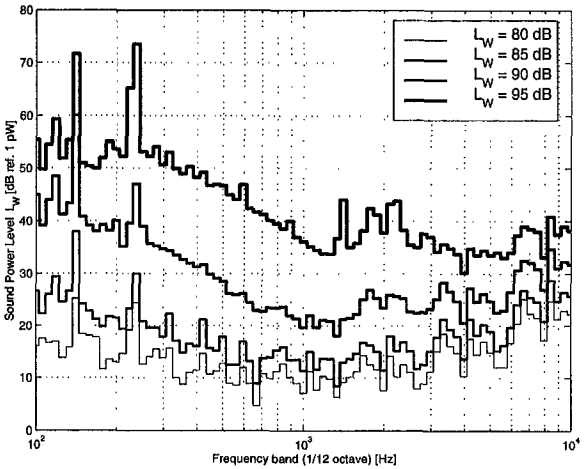

Figure 12: *Sound power of blowing sounds of a strongly converging-diverging port (port D) for the sound power levels 80, 85, 90 and 95 dB at the driving frequency. Physical port length L=0.13 m, Loudspeaker driven with a single frequency of 45 Hz.*

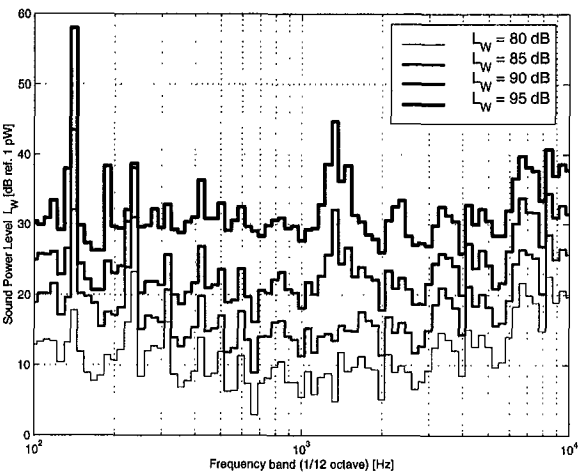

Figure 13: *Sound power of blowing sounds of a slowly converging-diverging port (port E) with curvature radii of 5 mm for the sound power levels 80, 85, 90 and 95 dB at the driving frequency. Physical port length L=0.13 m, Loudspeaker driven with a single frequency of 45 Hz.*

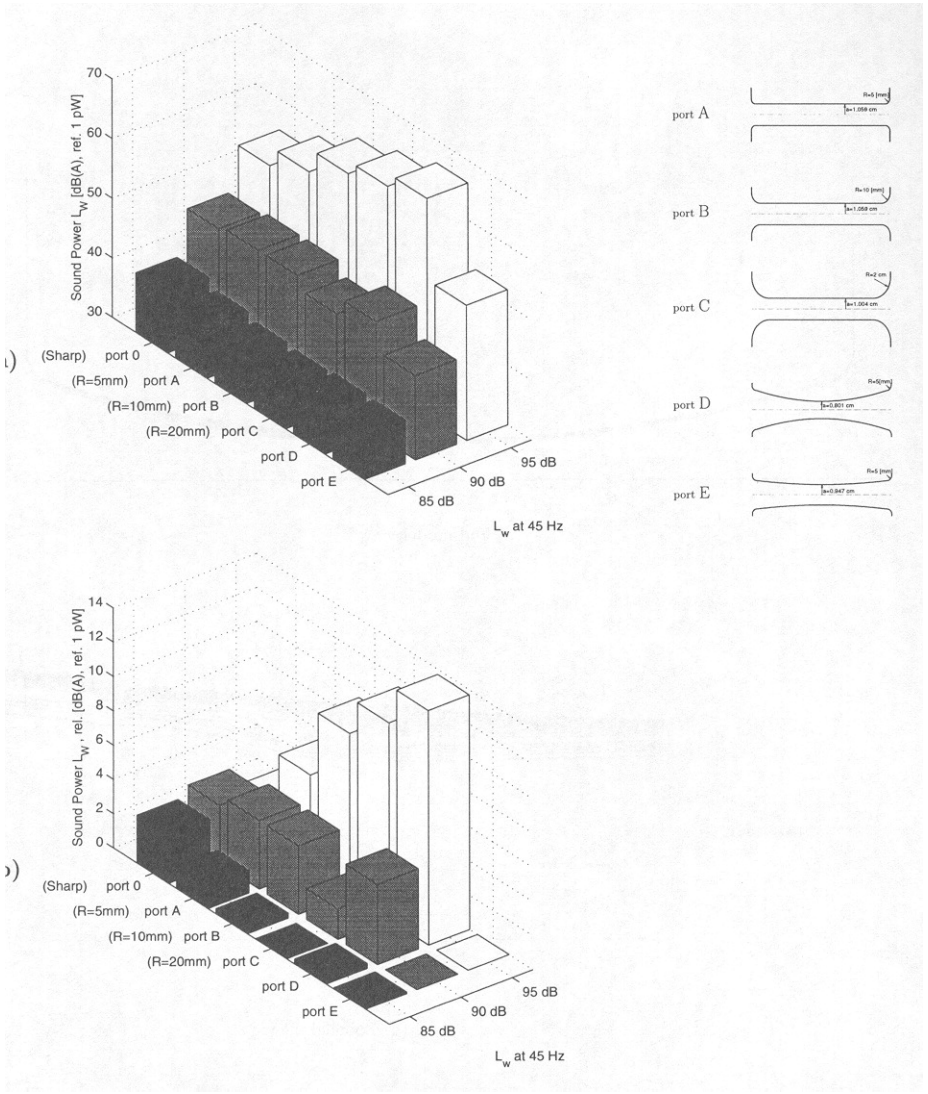

Figure 14: *Sound power of the blowing sounds for port 0, A, B, C, D and E, for equal sound pressure levels at the driving frequency at 1 m distance in an anechoic room,* **a)** *absolute sound power,* **b)** *sound power relative to port E.*